Electrostatic Properties of *N*-Acetyl-Cysteine-Coated Gold Surfaces Interacting with TiO₂ Surfaces

Jin-Won Park

Gachon Bionano Research Institute, College of Bionano Technology, Kyungwon University, Kyungki 461-701, Korea
E-mail: jwpark@kyungwon.ac.kr

It is found that that the coating *N*-acetyl cysteine (NAC) on gold surfaces may be used to design the distribution of either gold particle adsorbed to the TiO₂ surface or *vice versa* by adjusting the electrostatic interactions. In this study, we investigated electrostatic properties of the NAC-coated-gold surface and the TiO₂ surface. The surface forces between the surfaces were measured as a function of the salt concentration and pH value using the AFM. By applying the Derjaguin-Landau-Verwey-Overbeek (DLVO) theory to the surface forces, the surface potential and charge density of the surfaces were quantitatively acquired for each salt concentration and each pH value. The surface potential and charge density dependence on the salt concentration was explained with the law of mass action, and the pH dependence was with the ionizable groups on the surface.

Key Words: *N*-Acetyl cysteine, Gold surface, TiO₂ surface, AFM, DLVO theory

Introduction

Materials composed of gold and a semiconducting support such as TiO₂ are considered for numerous applications for example in surface patterning,[1] catalysis,[2-4] photocatalysis,[5] and photovoltaic cells.[6] In the latter case, the excitation of the semiconductor-metal nanocomposite by light induces electron-transfer processes that may be utilized for solar energy conversion,[7] *i.e.* for the production of hydrogen by water splitting. Activity and selectivity of such materials and catalysts rely on the distribution.[8]

Different approaches were used in the past to prepare Au-TiO₂ catalyst materials such as metal ion impregnation and deposition-precipitation followed by drying, calcinations, and reduction.[9] During such procedures the Au particles or clusters are formed directly on the support. However, these approaches have some disadvantages. The uneven precursor-solution loading due to gravitational forces leads to polydispersity of the resulting metal particles. The necessary thermal treatment furthermore results in severe agglomeration problems and may even cause chemical modification of the support through ionic diffusion.[5] Therefore, alternative routes for catalyst preparation are considered. A different approach relates to the preparation of metallic Au⁰ particles in solution and subsequent deposition on the TiO₂.[5,10] This approach is based on passivating ligands such as phosphines and thiols.[11,12] These ligands prevent the particles from agglomeration in solution. Once the gold particles are deposited on the TiO₂, the passivating ligands can be removed by calcinations of the material and thiolate oxidation.[4,13-15]

The atomic force microscope provides an ideal means to study directly the total force of interaction between a colloidal particle and a flat surface as a function of separation.[16] By fitting these force-separation curves with Derjaguin-Landau-Verwey-Overbeek (DLVO) theory,[17] it is possible to obtain the electrostatic properties of the surface being studied. These surface properties are an indicator to represent electrostatic repulsive force between particles, which may strongly affect on the particle distribution that is critical to the activity and selectivity of the catalyst. In this paper, we investigated electrostatic properties of the *N*-acetyl cysteine(NAC)-coated-gold surfaces and the TiO₂ surfaces.

Experimental

Surface preparation. The gold surfaces were prepared by using a high-vacuum electron beam evaporator to sequentially deposit a 5 nm chrome adhesion layer and a 100 nm gold layer on the silicon wafers. Immediately prior to use, the gold surfaces were cleaned in a 4:1 solution of 96% sulfuric acid and 30% hydrogen peroxide at 60-80 °C for 5 min. The gold surface was immersed in a solution of 10 mM NAC, 100 mM potassium nitride, at pH 4 for several hours at room temperature, followed by rinsing with a running buffer. The immobilization of NAC was confirmed from qualitative surface force measurement in 100 mM potassium nitride at pH 4. For quantitative surface force measurements, the solution was replaced with a running buffer (There are six running buffers used in this research − 100, 10, and 1 mM potassium nitride at pH 4 and 8, respectively). TiO₂ layer was deposited on the surface of the silicon wafer by sputtering titanium in an argon-oxygen environment for 41 min using an RF Magnetron source operating at 2 kW. Prior to sputtering, the wafers were dipped in hydrofluoric acid to remove any native oxide layer. The total pressure used was 5×10^{-6} bar, with argon and oxygen flow rates of 6 and 1.2 dm³/min, respectively. The substrate was rotated continuously during sputtering. The target to substrate distance was 7 cm and target diameter was 20 cm. The characteristics of the TiO₂ layers were identical with those of the gold surface.

AFM measurements. Topology images and surface force measurements were made with a 3-D Molecular Force Probe AFM (Asylum Research, Santa Barbara, CA) with a closed-loop piezo-electric transducer. Microfabricated silicon oxyni-
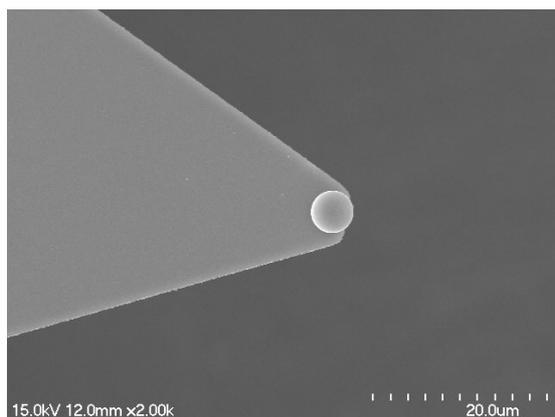
Figure 1. Titanium dioxide sphere-attached-cantilever.

tride cantilevers (Olympus, Shinjuku-ku, Tokyo, Japan) with a nominal radius of 20 nm were used for topographic imaging and qualitative surface force measurements. Quantitative surface force measurements were made with titanium oxide spheres (Microspheres-Nanospheres, Cold Spring, NY) of 3 μm diameter that were attached to the microfabricated cantilevers, shown in Figure 1. The spheres were immobilized at the end of the cantilever with UV-sensitive adhesive (Norland Products, New Brunswick, NJ). Exposure to the UV light source and surface cleaning were achieved in an ozone cleaning apparatus (Jelight, Irvine, CA). It was observed that the exposure did not cause any change in the response of the cantilever. The spring constant of the cantilever was determined from the thermal frequency spectrum of the cantilever.[18]

Theory

Theories describing the forces between interacting electrostatic double layers have been considered by numerous authors. The interaction between similarly charged double layers at low surface potentials lis described by the theory of DerjaguinLandau-Verwey-Overbeek(DLVO).[19] According to DLVO theory, the total interaction energy between two plates can be considered as the sum of several contributions, including an attractive van der Waals component(V_A) and an electrostatic repulsion or attraction(V_E). There is also considerable evidence for an additional repulsion(V_S) at close separations resulting from the presence of ordered solvent layers.[20-23]

Using the Derjaguin approximation,[24] the force between spheres of radius R_T can be related to the energy between plates by the expression

$$F / R_T = 2\pi(V_A + V_E + V_S) \quad (1)$$

The van der Waals energy (V_A) in the non-retarded limit is described by an equation of the form

$$V_A = -A_H / 12\pi d^2 \quad (2)$$

where A_H is the Hamaker constant and d is the separation distance.[25] The Hamaker constant of the NAC layer is assumed to be 7.0×10^{-20} J, since the most component of the layer is hydrocarbon.[26] The Hamaker constant used for the TiO₂ surface is 5.0×10^{-20} J.[27] The electrostatic interaction (V_E) can be derived by considering the free energy associated with the formation of a double layer or by integrating the electrostatic force.[28-30] Using the latter method, the interaction for a 1:1 Electrolyte is

$$V_E = -\int_{\infty}^{D}\left\{2n^0kT\left[\cosh\left(\frac{ze\psi}{kT}\right)-1\right]-\frac{\varepsilon}{2}\left(\frac{d\psi}{dz}\right)^2\right\}dz \quad (3)$$

where ψ is the electrostatic potential. The first term in eq 3 is a repulsive osmotic component that results from the accumulation of charge in the gap between the plates, and the second is a Maxwellian stress that represents an induced charge and is always attractive. For similarly charged surfaces, the second term disappears, leaving a results equivalent to DLVO. To determine V_E explicitly, the electrostatic potential must be known. This can be found by solving the Poisson-Boltzmann equation

$$\frac{d^2\psi}{dz^2} = -\frac{1}{\varepsilon_0\varepsilon_r}\sum_i n_i^0 z_i e \exp\left(-\frac{z_i e\psi}{kT}\right) \quad (4)$$

Generally, the complete nonlinear form of eq 4 must be solved, which can be accomplished only by numerical techniques.[31] Integration of eq 3 was then achieved with a Simpsons' 3/8 rule. The additional repulsive force (V_S) in eq 1 is thought to arise from the presence of ordered solvent layers and can be described by a decaying oscillatory force.[32] The nature of this repulsive force is not clearly understood and will be neglected in the calculations presented here.

Results and Discussion

The AFM was used to characterize the structures of the NAC layer formed on the gold surfaces. Constant force AFM images were acquired on the gold surfaces, NAC-coated gold surfaces, and TiO₂ surfaces. The morphologies of the gold surfaces, the NAC-coated gold surface, and the TiO₂ surfaces were dominated by the polycrystalline structure of the evaporated metals and had a roughness of 1.5 nm. Again, the morphologies of these surfaces were essentially indistinguishable (results were not shown). Phase separation in lipid and fatty acid films has been observed with AFM and is easily visualized as micrometer-sized domains in the contact imaging mode.[33] The fact that domains were not observed on the NAC-coated gold surfaces is strong evidence that the NAC forms homogeneous layer on the gold surfaces.

AFM force measurements were made on the gold surfaces and the NAC-coated gold surfaces with 20-nm-radius probes in order to confirm the formation of NAC layer on the gold surfaces. Figure 2 presents approaching force-distance measurements between a silicon nitride probe and the NAC layer formed in 100 mM potassium nitride at pH 4. The observed forces were purely short-range-repulsion below around 2.0
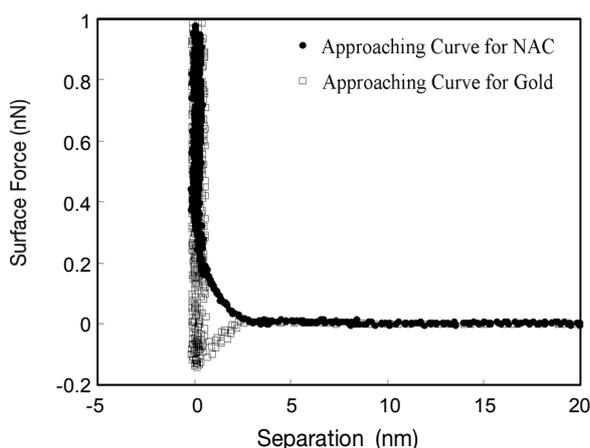
Figure 2. Force-distance curve between a silicon nitride probe and the *N*-acetyl-cysteine (NAC) layer formed in 100 mM potassium nitride at pH 4.
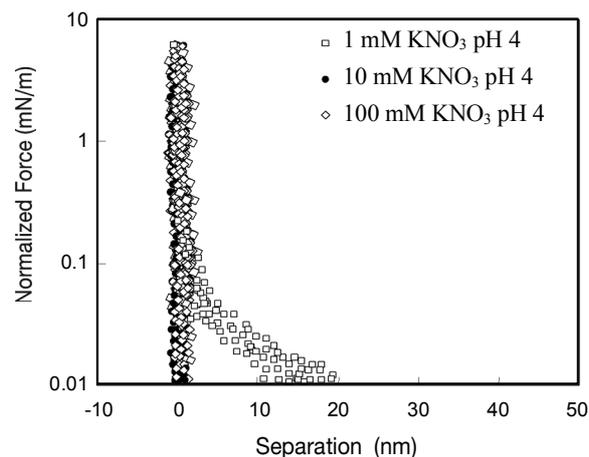

Figure 4. Approaching force curve as a function of the separation between the sphere and the surface of the titanium dioxide in 1, 10, 100 mM potassium nitride at pH 4.
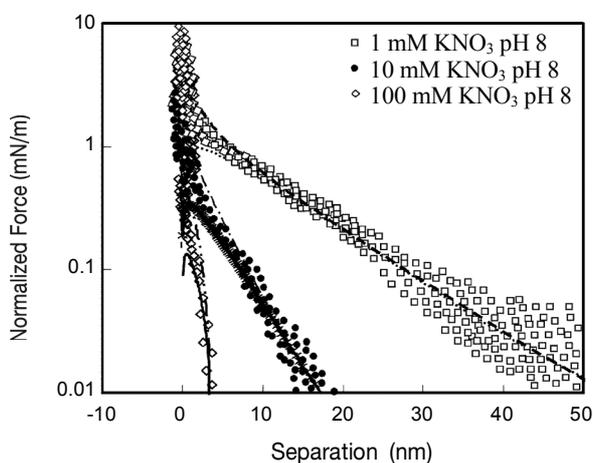

Figure 3. Approaching force curve as a function of the separation between the sphere and the surface of the titanium dioxide in 1, 10, 100 mM potassium nitride at pH 8.

nm at loads of approximately 0.2 nN, while the force curve of the gold surface showed an attractive region. The repulsion, not found on the gold surfaces, appears to be due to the lower Hamaker constant and more hydration of the NAC layer.[26] The clear difference of the force curve indicates that the NAC layers were well-formed on the gold surfaces.

For the quantitative characterization of the NAC-coated-gold surface properties, the surface charge density and potential of the 3-μm-diameter titanium dioxide sphere were found as a first with the force measurements between the sphere and the titanium dioxide surface. Figure 3 shows the approaching surface force measurements as a function of the separation between the titanium dioxide sphere and the titanium dioxide surface in three running buffers at pH 8. The long-range surface forces were purely repulsive, and their range was highly dependent on the ionic strength of the solution. The exponential dependence of the repulsive force on distance was consistent with double-layer forces between surfaces of like charge in aqueous solutions. At separations of less than 2

nm, significant short-range repulsive forces were observed that may be attributed to the steric forces and the inherent roughness of the surfaces.[34,35] However, the behavior of surface forces at pH 4 was different from that at pH 8. Figure 4 shows the force curves made at pH 4. The repulsive forces, observed in 1 mM potassium nitrate solution at pH 4, were smaller than those at pH 8 due to the iso-electric point of TiO$_2$. The forces were not found in 10 mM and 100 mM potassium nitrate solution at pH 4. That is, in 10 mM and 100 mM potassium nitrate solution at pH 4, the electrostatic forces in the long range appeared not to be the dominant component of the surface forces on the TiO$_2$ surface. Therefore, in 10 mM and 100 mM potassium nitrate solution at pH 4, it was not appropriate to apply the DLVO theory to the force curves so that the surface potential and charge density could be acquired.

The DLVO theory was applied to analyze the long-range surface forces using either constant surface potential or charge density boundary conditions. The results of these calculations are summarized in Table 1. The surface potential of the titanium dioxide surface is on the order of -10 to -100 mV at pH 8.0. Our results appear to be consistent with those of Feiler *et al.*,[27] where AFM was used to characterize the charge state of the titanium dioxide surface in a 1 mM potassium nitrate solution and the surface potential was found to be -43 mV at pH 8. The change from negative potential to positive potential is due to change from negative to positive values at an isoelectric point of pH 4.3.[27] For the 10 mM and 100 mM potassium nitrate solution at pH 4, the surface potential and charge density of the TiO$_2$ were not acquired.

From Table 1, it can be seen that the surface potential of the titanium dioxide surface increased monotonically with decreasing ionic strength and that the surface charge density deceased monotonically with decreasing ionic strength at pH 8. Pashley has developed a model to explain the salt concentration dependence of the surface potential and charge density of a surface with ionizable groups based on the law of mass action.[36] The interrelation between surface charge density (σ), surface potential (ψ_o), and salt concentration may be determined by the simultaneous solution of the law of mass action

Table 1. Electrostatic properties of the titanium dioxide surfaces

	pH 8		
	1 mM Potassium nitrate	10 mM Potassium nitrate	100 mM Potassium nitrate
Surface potential (mV)	-42 ± 4	-27 ± 3	-18 ± 2
Surface charge density (10^{-3} C/m²)	-3.0 ± 0.3	-6.8 ± 0.6	-12.5 ± 1.3
	pH 4		
	1 mM Potassium nitrate	10 mM Potassium nitrate	100 mM Potassium nitrate
Surface potential (mV)	$+10 \pm 1$	-*	-*
Surface charge density (10^{-3} C/m²)	$+0.7 \pm 0.2$	-*	-*

*Electrostatic property was not acquired.
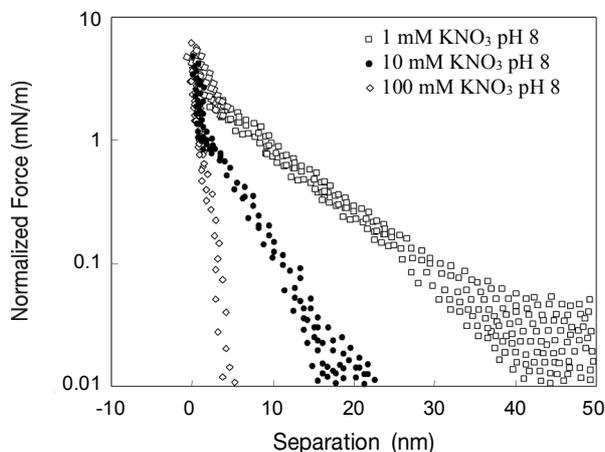
Figure 5. Approaching force curve as a function of the separation between the titanium dioxide sphere and the NAC layer in 1, 10, 100 mM potassium nitride at pH 8.

$$\sigma = \sigma_o \frac{1}{1 + K_a [H^+] \exp\left(-\dfrac{e\psi_o}{kT}\right) + K_{Na^+}[Na^+]\exp\left(-\dfrac{e\psi_o}{kT}\right)} \qquad (5)$$

and Graham's equation

$$\sigma = \sqrt{8\varepsilon\varepsilon_o kT}\, \sinh\left(\frac{e\psi_o}{kT}\right)\, \sqrt{([Na^+] + [H^+])} \qquad (6)$$

where σ_o is the maximum surface charge density, ψ_o is the surface potential, ε is the dielectric constant of water, ε_o is the permittivity of free space, e is the electronic charge constant, k is the Boltzmann's constant, T is temperature. The surface potential and charge density dependence on the salt concentration measured at pH 8.0 were consistent with the trends predicted by Pashley's model. For the purpose of this study, the experimentally measured titanium dioxide surface potential and charge density were used to characterize the NAC layer formed on the gold surfaces.

The surface potential and charge density of the NAC layer formed on the gold surfaces were characterized by making
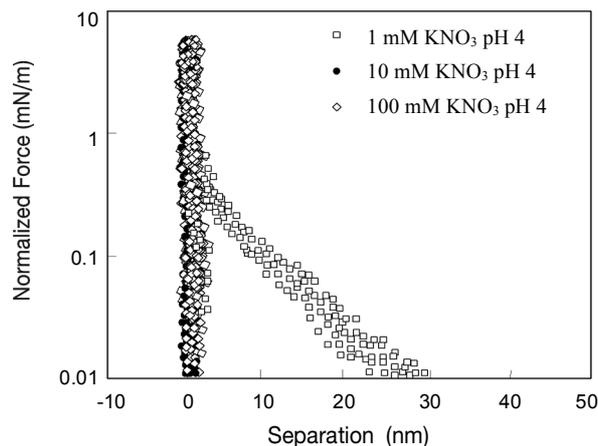
Figure 6. Approaching force curve as a function of the separation between the titanium dioxide sphere and the NAC layer in 1, 10, 100 mM potassium nitride at pH 4.

surface force measurements on them with the titanium dioxide sphere. Figure 5 shows the results of force measurements made on the NAC layers in the three running buffers at pH 8. The long-range surface forces were purely repulsive and varied in range with ionic strength in a manner that was consistent with double-layer forces. Quantitative analysis of the surface forces with the DLVO theory was performed using asymmetric boundary conditions. Table 2 summarizes the surface potentials and charge densities measured on the NAC layers as a function of ionic strength and pH value. The surface potential and charge density dependence of the NAC layer on the salt concentration were also consistent with Pashley's model. It was observed that the surface charge densities and potentials of the NAC layer were much larger than those for the titanium dioxide surfaces at pH 8, which can be attributed to the ionized-functional-groups of the NAC layer. The long range forces were purely attractive in 1 mM potassium nitrate solution at pH 4, as shown in Figure 6. This phenomenon was predictable, considering pK$_a$ of the NAC and the iso-electric point of TiO₂. The long range forces were not observed in 10 mM and 100 mM potassium nitrate salt concentrations at pH 4, which was consistent with the fact that there were no long range forces on the TiO₂ surfaces.

The observations described above suggest that the electrostatic forces between the NAC-coated gold surfaces and TiO₂ surfaces were found to be adjustable quantitatively with a salt concentration and pH value. This fact led us to believe that the kinetics of the adsorption for either TiO₂ particles to NAC-coated-gold surface or NAC-coated-gold particles to TiO₂ surface might be also adjustable, because the adsorption is determined by the surface forces between the surfaces. Furthermore, the kinetics is related to the distribution of the particles adsorbed to the surface. Therefore, the surface forces as a function of the salt concentration and the pH value seem to be important for the design of the distribution of the particles adsorbed to the surfaces, which can affect on the efficiency of catalysts.

In conclusion, the surface forces between the NAC-coated-gold surface and the TiO₂ surface were measured as a function

Table 2. Electrostatic properties of the *N*-acetyl-cysteine (NAC) layer

	pH 8		
	1 mM Potassium nitrate	10 mM Potassium nitrate	100 mM Potassium nitrate
Surface potential (mV)	-85 ± 7	-53 ± 5	-34 ± 3
Surface charge density (10^{-3} C/m²)	-15 ± 2	-27 ± 3	-49 ± 5
	pH 4		
	1 mM Potassium nitrate	10 mM Potassium nitrate	100 mM Potassium nitrate
Surface potential (mV)	-22 ± 2	-**	-**
Surface charge density (10^{-3} C/m²)	-1.8 ± 0.2	-**	-**

**Electrostatic property was not acquired.

of the salt concentration and pH value using the AFM. By applying the DLVO theory to the surface forces, the surface potential and charge density of the surfaces were quantitatively acquired for each salt concentration and each pH value. The surface potential and charge density dependence on the salt concentration was explained with the law of mass action, and the pH dependence was with the ionizable groups on the surface. This study demonstrated that the coating *N*-acetyl cysteine on gold surfaces may be used to design the distribution of either gold particle adsorbed to the TiO₂ surface or vice versa by adjusting the electrostatic interactions.

References

1. Sun, S. Q.; Mendes, P.; Critchley, K.; Diegoli, S.; Hanwell, M.; Evans, S. D.; Leggett, G. J.; Preece, J. A.; Richardson, T. H. *Nano Lett.* **2006**, *6*, 345.
2. Haruta, M.; Kobayashi, T.; Sano, H.; Yamada, N. *Chem. Lett.* **1987**, *2*, 405.
3. Haruta, M.; Yamada, N.; Kobayashi, T.; Iijima, S. *J. Catal.* **1989**, *115*, 301.
4. Chou, J.; McFarland, E. W. *Chem. Commun.* **2004**, *14*, 1648.
5. Li, J.; Zeng, H. C. *Chem. Mater.* **2006**, *18*, 4270.
6. Tian, Y.; Tatsuma, T. *J. Am. Chem. Soc.* **2005**, *127*, 7632.
7. Kamat, P. V. *J. Phys. Chem. C* **2007**, *111*, 2834.
8. Valden, M.; Lai, X.; Goodman, D. W. *Science* **1998**, *281*, 1647.
9. Sakurai, H.; Tsubota, S.; Haruta, M. *Applied Catalysis A-General* **1995**, *102*, 125.
10. Li, X.; Fu, J.; Steinhart, M.; Kim, D. H.; Knoll, W. *Bull. Korean Chem. Soc.* **2007**, *28*, 1015.
11. Schmid, G. *Chem. Rev.* **1992**, *92*, 1709.
12. Noh, J.; Park, H.; Jeong, Y.; Kwon, S. *Bull. Korean Chem. Soc.* **2006**, *27*, 403.
13. Dasog, M.; Scott, R. W. J. *Langmuir* **2007**, *12*, 3381.
14. Sandhyarani, N.; Pradeep, T. *Chem. Phys. Lett.* **2001**, *338*, 33.
15. Brewer, N. J.; Rawsterne, R. E.; Kothari, S.; Leggett, G. J. *J. Am. Chem. Soc.* **2001**, *123*, 4089.
16. Binnig, G.; Quate, C.; Gerber, G. *Phys. Rev. Lett.* **1986**, *56*, 930.
17. Derjaguin, B. V.; Landau, L. *Acta Physiochem.* **1941**, *14*, 633.
18. Cleveland, J. P.; Manne, S.; Bocek, D.; Hansma, P. K. *Rev. Sci. Instrum.* **1993**, *64*, 403.
19. Derjaguin, B. V. *Trans. Faraday Soc.* **1940**, *36*, 203.
20. Israelachvili, J. N.; Adams, G. E. *J. Chem. Soc. Faraday Trans.* **1978**, *74*, 975.
21. Shuin, V.; Kekicheff, P. *J. Colloid Interface Sci.* **1993**, *155*, 108.
22. Parker, J. L.; Christenson, H. K. *J. Chem. Phys.* **1988**, *88*, 8013.
23. O'Shea, S. J.; Welland, M. E.; Pethica, J. B. *Chem. Phys. Lett.* **1994**, *223*, 336.
24. Derjaguin, B. V. *Kolloid Z.* **1934**, *69*, 155.
25. Hartmann, U. *Phys. Rev. B* **1991**, *43*, 2404.
26. Israelachivili, J. N. *Intermolecular & Surface Forces*; Academic Press: New York, 1991; pp 183-188, 275-282.
27. Feiler, A.; Jenkins, P.; Ralston, J. *Phys. Chem. Chem. Phys.* **2000**, *2*, 5678.
28. Verwey, E. J. W.; Overbeek, J. T. G. *Theory of the Stability of Lyophobic Colloids*; Elsevier: New York, 1948; pp 51-63.
29. Hogg, R.; Healy, T. W.; Fuerstenau, D. W. *Trans. Faraday Soc.* **1966**, *62*, 1638.
30. Hunter, R. J. *Foundations of Colloid Science*; Oxford University Press: Oxford, U. K., 1987; pp 397-409.
31. Chan, D. Y. C.; Pashley, R. M.; White, L. R. *J. Colloild Interface Sci.* **1980**, *77*, 283.
32. Parker, J. L. *Surf. Sci.* **1994**, *3*, 205.
33. Park, J.-W.; Ahn, D. J. *Colloids & Surf. B: Biointerf.* **2008**, *62*, 157.
34. Ducker, W. A; Senden, T. J.; Pashley, R. M. *Nature* **1991**, *353*, 239.
35. Horn, R. G.; Smith, D. T.; Haller, W. *Chem. Phys. Lett.* **1989**, *162*, 404.
36. Pashley, R. M. *J. Colloid Interface Sci.* **1981**, *83*, 531.